

## Manufacture of Clay Aggregate Doped with Pozzolan Destined for Lightweight Concrete

Hamza Mesrar<sup>1</sup>, Laila Mesrar<sup>2\*</sup>, Abdelhamid Touache<sup>3</sup>, Raouf Jabrane<sup>1</sup>

<sup>1</sup> Laboratory of Intelligent Systems, Georesources and Renewable Energies, Geology Department, Sidi Mohamed Ben Abdellah University, Fes, Morocco

<sup>2</sup> Laboratory Waves and Complex Environnement, Normondie University, UMR 6294 CNRS, France

<sup>3</sup> Laboratory of Mechanical Engineering, Mechanical Department, Sidi Mohamed Ben Abdellah University, Fes, Morocco

\* Corresponding author's e-mail: hamza.mesrar@usmba.ac.ma

### ABSTRACT

In this work, marl clay was used because these materials have a very important industrial potentiality in several fields, namely ceramics. The objective was manufacturing expanded clay aggregate (ECA), with two main ingredients of marl and pozzolan at different percentages in order to integrate them into the concrete as aggregate. The physicochemical parameters of the mixture marl / Pozzolan was discussed and the results of the analyses, allowed deducing that the sample with 15% pozzolan has the most expansion rate of 16.8%, and its density of 1232 kg/m<sup>3</sup> is in accordance with the international standard of expanded aggregates. The density of the concrete decreases with the quantity of ECA added and reaches its minimum with 1671 kg/m<sup>3</sup> according to concrete with 50% of the expanded aggregate. The bending tests show the increase of the mechanical strength as a function of the quantities of aggregate added. The results show a very important potential with the addition of clay aggregates, density and water absorption decrease with the increase of the mechanical resistance.

**Keywords:** marl, pozzolan, density, expanded clay aggregate, concrete, mechanical resistance.

### INTRODUCTION

In recent years, there is an increasing demand for granular materials used in the construction sector in Morocco, the depletion of natural reserves is a matter of time, these intense extractions of aggregates made along the beds of rivers or natural sand beaches destabilize the geomorphological and biological balance of the aquatic ecosystem. The preservation of ecosystems by reducing the intense extraction of natural environments and energy savings in order to reduce the emission of greenhouse gases has become paramount.

The study area is the quarry that is located in northwest Morocco, along the outer limit of the southern Rifan Range at the contact of the Sais Basin, which consists mainly of chaotic-structured gravity nappes resulting from the destruction of outward moving nappe fronts [Leblanc

and Olivier, 1984]. The samples were collected northwest of the city of Fez and are composed mainly of an Upper Miocene marl matrix [Tejera De Leon et al., 1995]. Marl is a type of clay found on the surface or at depth in the form of sediments or unconsolidated rocks, it is composed mainly of clay minerals and limestone [Durand, 1972]. Clay minerals are formed by physical or chemical alteration of the silicon and aluminum rich parent rock and reveal an amazing diversity of mineralogical composition as they exhibit a wide range of solid solutions and a great ability to form mixed crystals by interstratification [Reynolds, 1980]. The large reserve of this material and its ease of surface extraction make it very important for industrial exploitation. Its physical properties such as its plasticity and interesting refractory clay minerals give it a very interesting exploitation potential [Grim, 1953].

It is used for various industrial applications (ceramics, inks, purification oils, pharmaceuticals, paper, paint, oil industry, etc.). Clay is one of the most used industrial raw materials, the latest studies on the Miocene marls of Benjalik show an impressive potential, and they have been doped with  $MnO_2$ ,  $Fe_2O_3$ , and  $Al_2O_3$  [Mesrar et al., 2014, 2021]. Conventional concrete is very expensive, and causes irreparable damage to the environment, hence the idea of preparing a thermal insulation material with acceptable mechanical properties [Yew et al., 2021]. Clay is used as a construction product by preparing Expanded Clay Aggregate (ECA), either by clays like vermiculite which has a very high expansion capacity [Becker et al., 2022], or by polypropylene fibers, which have a very low density [Yew et al., 2021; Ye et al., 2022], and then their incorporation in lightweight concrete [Zhang et al., 1992; Wasserman and Bentur, 1997].

On the other hand, the marl shrinks with the increase of temperature because the porosity created during the firing enables the gases released by the decomposition of carbonates and organic matter to escape [Allison et al., 1965]. This is why the authors had the idea of adding pozzolan because iron and quartz close the pores of the surface with a phenomenon called vitrification [Akwilapo et al., 2003], to store the gases and obtain the expansion of the aggregates. Marls were mixed with 10%, 15% and 20% pozzolan to know the percentage that gives the greatest expansion and specifying the temperature and time necessary for firing. The addition of calcium and aluminum powder [Azarhomayun et al., 2022], metakaolin and silica fume [Güneyisi et al., 2012] were used in previous studies.

In the formulation of concrete, others use fly ash [Wasserman and Bentur, 1997] or rice husk ash and coal bottom ash [Bheel et al., 2021] or newsprint ash [Wong et al., 2022], and they have also studied the physicochemical properties [Khudhair et al., 2018; Khudhair et al., 2017], thermal parameters, microstructural and acoustic parameters [Becker et al., 2022], fire resistance [Alireza et al., 2021], or have conducted research on the pre-wetting of clay aggregates and its effect on durability [Musial et al., 2021], liquefaction attenuation [Ghorbani et al., 2021] and also on the flexural strength of lightweight concrete [Baronet et al., 2022]. The lightweight concrete mix was performed according to the world standards as it has been done in several studies before [Melanie,

2003; Bogas et al., 2014]. Then, it was monitoring during curing by measuring the shrinkage of concrete until the curing age of 28 days [Baronet et al., 2022]. After curing, the study of physical properties, such as density [Wang et al., 2022], water absorption [Zheng et al., 2021] and mechanical characteristics using three-point bending strength was carried out [Azarhomayun et al. 2022; Baronet et al., 2022].

## MATERIALS AND METHODS

### Samples preparation

In the present study, the used marl originated from Quarry of Ben Jallik, Fez, Morocco (Fig. 1). The marl samples were oven dried at  $105^\circ C$  for 24 hours, quartered to select a representative sample of the materials. Then, they were manually ground to a reduced particle shape. Subsequently, they were finely ground for 5 minutes in an agate mill, and doped the marls with pozzolan at different percentages (0%, 10%, 15%, and 20%). Afterwards, the mixture was ground for 5 minutes to better homogenize the materials. The expanded clay aggregate is prepared by the composite of marl/pozzolan with an addition of water. The light aggregate was dried in the oven at  $105^\circ C$  for 24 hours to start the firing process in a muffle furnace for 5, 10, 15, 30 minutes, to evaluate the expansion of ECA, on each temperature, namely  $900\text{--}1100^\circ C$  in  $100^\circ C$  increment (Fig. 2). Then, the higher expansion aggregate with cement (CPG45) and sand was used, to formulate the lightweight concrete according to the procedure described in NF EN 133699 (Fig. 3).

### Chemical analysis

The chemical composition of clays was determined by X-ray and fluorescence spectrometry (Axios, ELE03-PROT v01) using pressed powder pellets. For X-ray fluorescence, irradiation with a primary X-ray bundle from an X-ray tube causes the emission of fluorescent x-rays with discrete energies characteristic of the elements present in the sample. The analysis were performed at the National Center for Scientific and Technological Research (NCSTR) (Morocco).

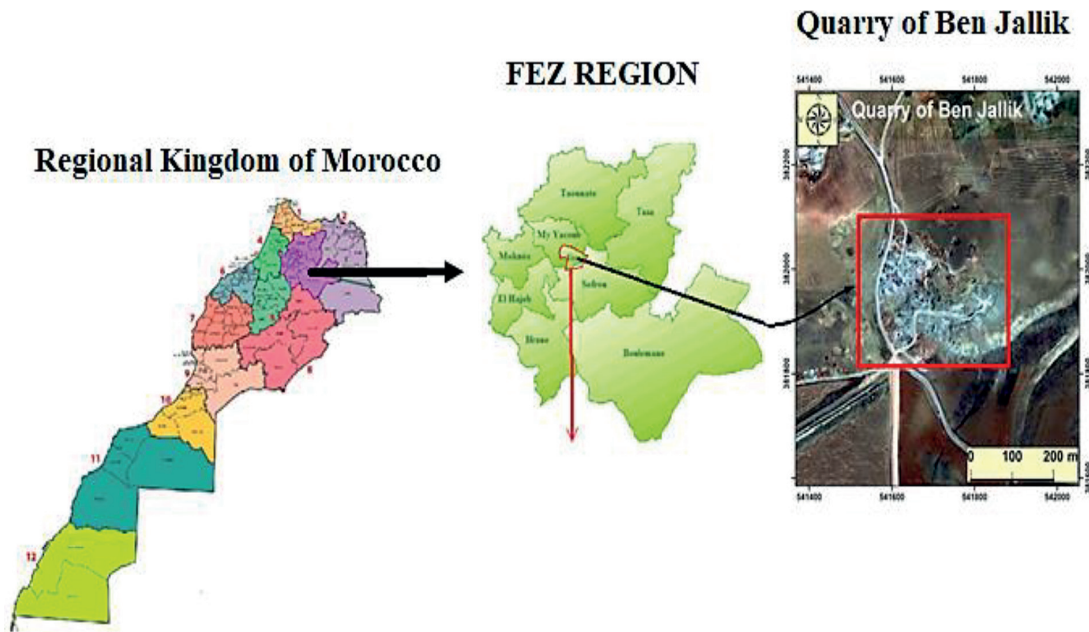


Figure 1. Location of the sites investigated (Quarry of Ben Jallik, Fez, Morocco)

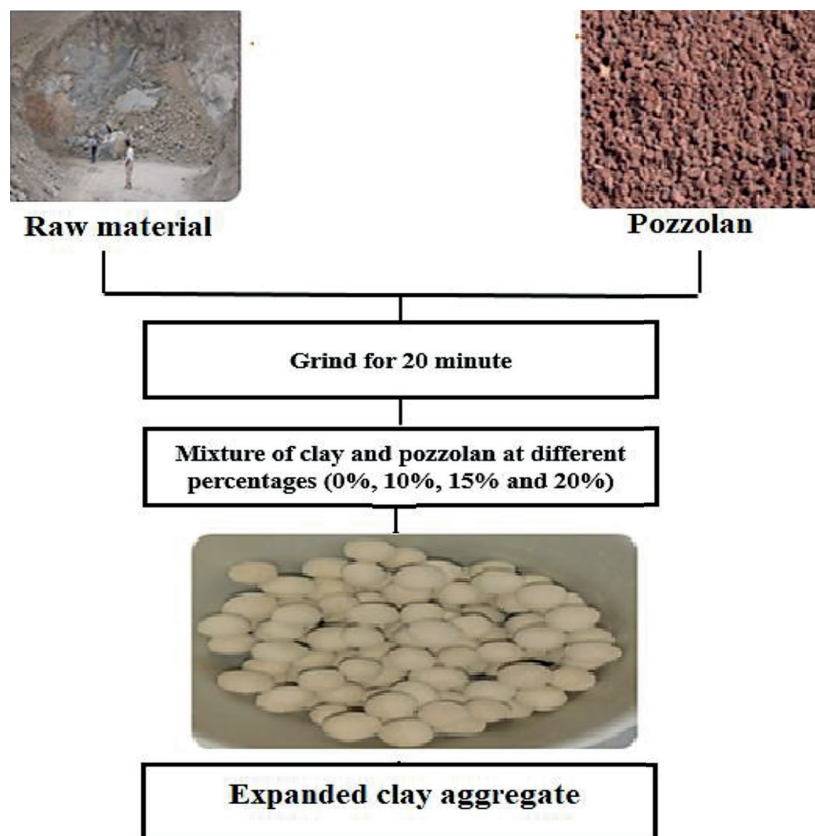


Figure 2. The schematic process of composite material

### Physical analysis

#### Scanning electron microscope (SEM)

The SEM image is effected by a pressure controlled instrument, the cathode which produces

the electron beam, the condenser system which forms a reduced image of the cross-over which is then projected by an objective lens on the object, the scanning system formed by the deflection coils to move the probe on the object and finally

the detector which picks up the signals coming from a fluorescent screen and produces a black and white image.

#### Atterberg limits

The Atterberg limits are a basic measure of the critical water contents of a fine-grained soil: its plastic limit, and liquid limit. The test is obtained by using standard (NF P 94-051).

#### Differential scanning calorimetry (DSC)

Thermoanalytical technique in which the difference in the amount of heat required to raise the temperature of a sample and a reference is measured as a function of temperature. The sample and reference are kept at approximately the same temperature throughout the experiment. In general, the temperature program for a DSC analysis is designed, so that the temperature of sample holder increases linearly with time. The reference sample must have a well-defined heat capacity over the temperature range to be analyzed.

#### Density

The procedure for measuring density is essentially based on mass and volume of sample, which is placed in a small cup (pycnometer) of known volume at a given temperature. In order to calculate the density, the weight obtained was taken and divided by the volume of the liquid tested.

#### Water absorption

This test was performed on hardened concrete and water absorption was measured by immersion using international standard (NBN B 15-215(1989)). This test gives some information about the porosity and consequently the resistance of the material.

#### Mechanical analysis

The bending strength tests were realized in the mechanical laboratory of FST Fez. Testing was carried out by W500 machine (Fig. 4), with a maximum effort of 50 KN and connected to a software-driven computer system (EM 506), which gives the evolution of the bending resistance (N) according to the displacement (mm). To calculate the maximum resistance of flexural strength, the equation of three point bending was used [Bogas et al., 2014]:

$$\sigma_{max} = \frac{3}{2} \left( \frac{FL}{bd^2} \right) \quad (1)$$

The results are expressed in MPa. The flexural strength is tested for the comparison between fired and unfired bricks.

## RESULTS AND DISCUSSION

### Chemical composition

The chemical composition of the marls is shown in (Tables 1 and 2), it is formed by 46.6% of SiO<sub>2</sub> (it has an effect of refractoriness and contraction of the mass) [Kornmann et al., 2005]; 13.4% Al<sub>2</sub>O<sub>3</sub> (the fact that these marls contain 15% of Al<sub>2</sub>O<sub>3</sub> means that they are considered moderately plastic); 8.87% CaO (it influences the porosity of the material and its presence indicates that the mineral contains plagioclases); 6.91% Fe<sub>2</sub>O<sub>3</sub> (which acts as a flux; this oxide is the cause of the brown or red color of the products after firing) [Arib et al., 2007]; 19.9% of loss on ignition and 4.32% of minor elements (P<sub>2</sub>O<sub>5</sub>; MnO; Na<sub>2</sub>O; K<sub>2</sub>O; MgO and Cl) they promote the formation of a glassy phase with a low melting point during the firing process (energetic flux role). From these results, it can be concluded that these marls can be used in ceramics [Nshimiyimana et al., 2020]. It was noticed that the addition of pozzolan leads to an increase in the rate of iron and titanium oxides and a decrease in the loss on ignition.

### Physical analysis

#### Scanning electron microscope

The SEM gives the magnified images of the size, shape, composition, crystallography, and other physical and chemical properties of a specimen. The raw sample presented in (Fig. 6) shows quartz grains and phyllosilicate in sheet form, while the sample doped with 15% pozzolan shows a significant structural change (Fig. 7), notably an increase in closed porosity compared to the raw sample.

#### Atterberg limits

The curve presents the limits of Atterberg as a function of the percentage of pozzolan, indeed, the addition of pozzolan in marls introduces an increase in plasticity and a decrease in the limit of liquidity [Pimraksa et al., 2009; Silva et al., 2014], which reveals that the pozzolan plays a

role of degreaser and contributes to the phenomenon of the expansion [Ainete et al., 2006; James et al., 2018] (Fig.8).

#### Differential scanning calorimetry

The differential calorimetry curves represent the variation of the absorbed energy as a function of time (Fig. 9). The results show the decrease

in absorbed thermal energy with the amount of pozzolan added. It is obvious that the effect of the pozzolan has modified the thermal properties of the marl. Therefore, the material becomes more insulated with the addition of the pozzolan. On the industrial level, this parameter is of great use on the economic level of the energy in particular in the building and public works sector (BPWS).

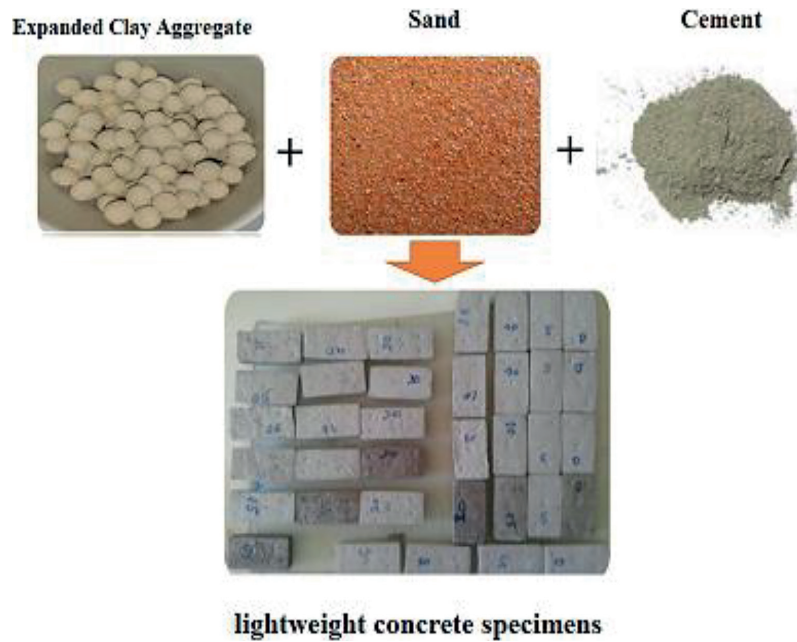


Figure 3. The schematic process of lightweight concrete

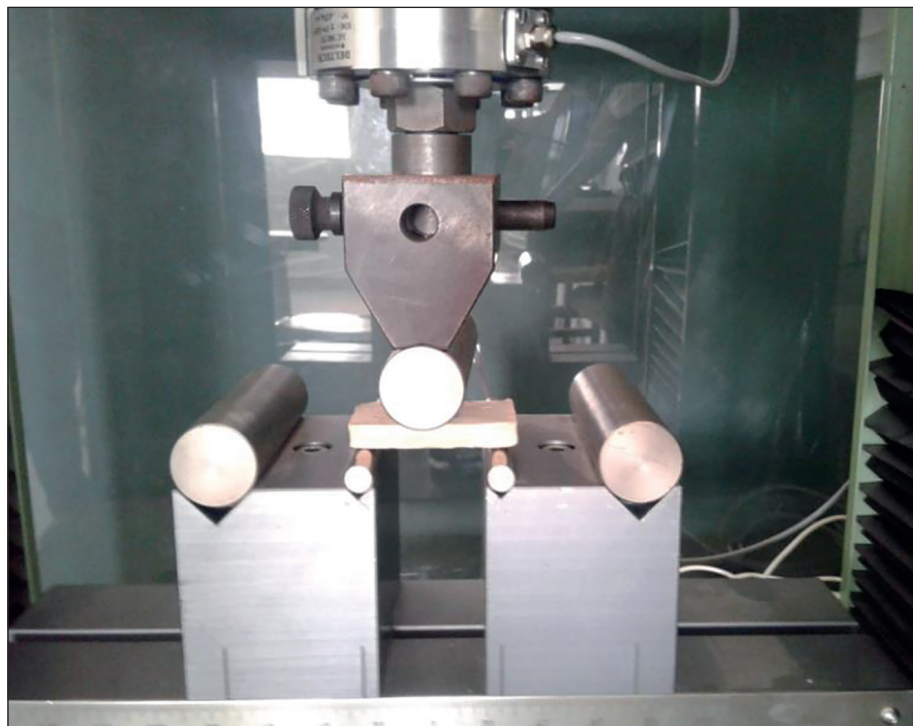


Figure 4. Photographs of the flexural strength machine (W500)

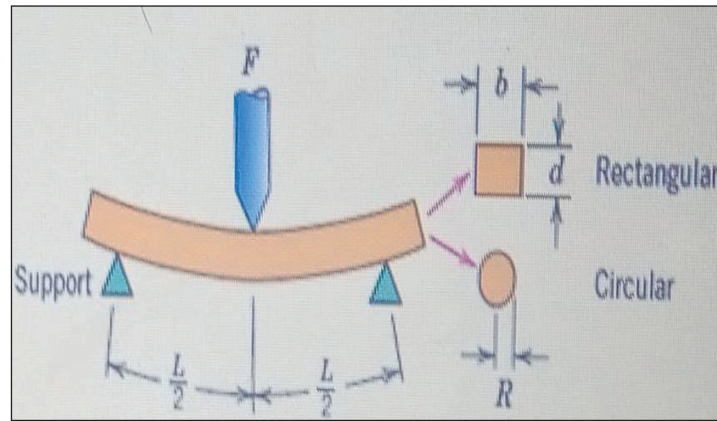


Figure 5. Arrangement of specimen for flexural strength test.

Table 1. Chemical component analyses of raw and mixed materials (Wt. %)

Percentages of pozzolan in the raw material	SiO <sub>2</sub>	L.O.I	Al <sub>2</sub> O <sub>3</sub>	CaO	Fe <sub>2</sub> O <sub>3</sub>	MgO	Cr <sub>2</sub> O <sub>3</sub>	Na <sub>2</sub> O	K <sub>2</sub> O	SO <sub>3</sub>	TiO <sub>2</sub>	NiO	P <sub>2</sub> O <sub>5</sub>	MnO <sub>2</sub>	Cl
0%	40.6	19.9	13.4	8.87	6.91	3.44	2.16	1.58	1.19	0.629	0.355	0.234	0.207	0.206	0.165
15%	40.7	18.8	13.5	8.65	7.9	3.43	2.27	1.37	1.17	0.586	0.525	0.262	0.244	0.273	0.156
20%	39.9	18.8	13.3	8.71	8.41	3.62	2.34	1.39	1.07	0.589	0.58	0.288	0.279	0.247	0.156

Table 2. Fluorescence analysis of Pozzolan

Oxides names	Concentrations (%)
SiO <sub>2</sub>	37.8
Al <sub>2</sub> O <sub>3</sub>	17.0
Fe <sub>2</sub> O <sub>3</sub>	17.3
MgO	6.2
CaO	3.88
Na <sub>2</sub> O	0.82
K <sub>2</sub> O	0.355
P <sub>2</sub> O <sub>5</sub>	0.72
TiO <sub>2</sub>	2.3
NiO	0.47
MnO <sub>2</sub>	0.435
Cr <sub>2</sub> O <sub>3</sub>	2.87
SO <sub>3</sub>	0.33
Cl	0.16
Loss on ignition	9.00

### Firing process

The curves show that the aggregate diameter increases with firing time, since pozzolan intensifies the porosity [Matias et al., 2014] and reduces the pore size [Li et al., 2020]. The raw sample reveals an increase in the expansion rate with time and reaches its maximum at 6.25% around 30 min. However, the diameter of the expanded clay aggregate doped with 15% and 20% pozzolan

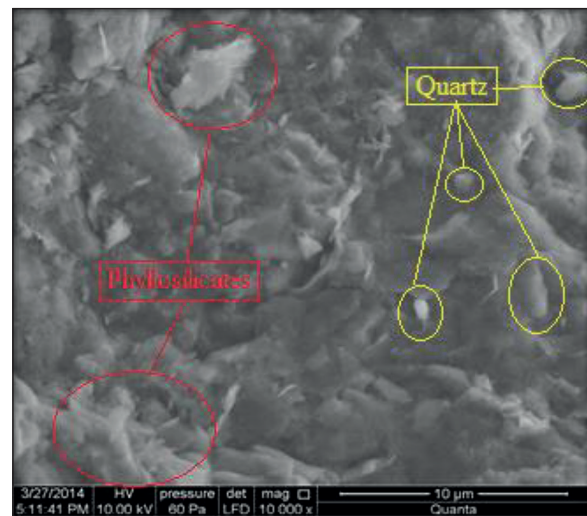


Figure 6. SEM image of clay used in the formulation

shows significant expansion at 30 min (Fig. 10). The highest expansion rate which reaches 16.8% for (15% PZL) with a density of 1232 kg/m<sup>3</sup> in agreement with other authors [Nie et al., 2011; Mydin et al., 2015], shows an interest for its use in lightweight concrete [Wasserman and Bentur, 1997; Bogas et al., 2014].

### Density of concrete

Indeed, lightweight concrete is less heavy than conventional concrete. It can be placed on

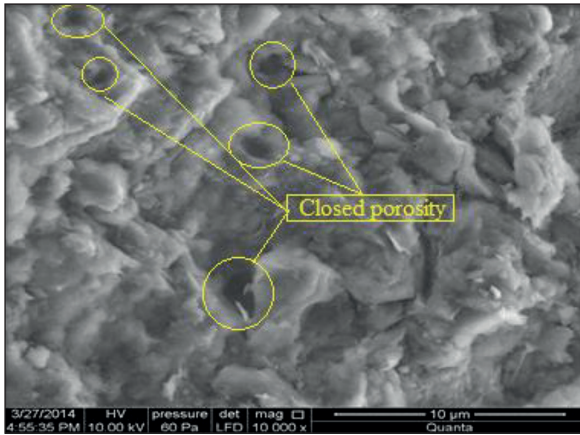


Figure 7. SEM image of formulation clay and 15% of pozzolan

a structure requiring a lower load resistance. This can be an advantage because the structure is easier to put in place and consequently, savings are made. In addition to its low density, lightweight concrete has the particularity of being both a good thermal and sound insulator (Fig. 11).

For the placement of lightweight concrete, the authors complied with the NF EN 13369 (2013) standards. For 1 volume of cement + 2 volume of sand + % of EC). The results show a negative correlation between density and the proportion of expanded clay aggregate added in the concrete samples (Fig. 9). The employed ECA marl and pozzolan achieved the desired objective since the densities of the concretes

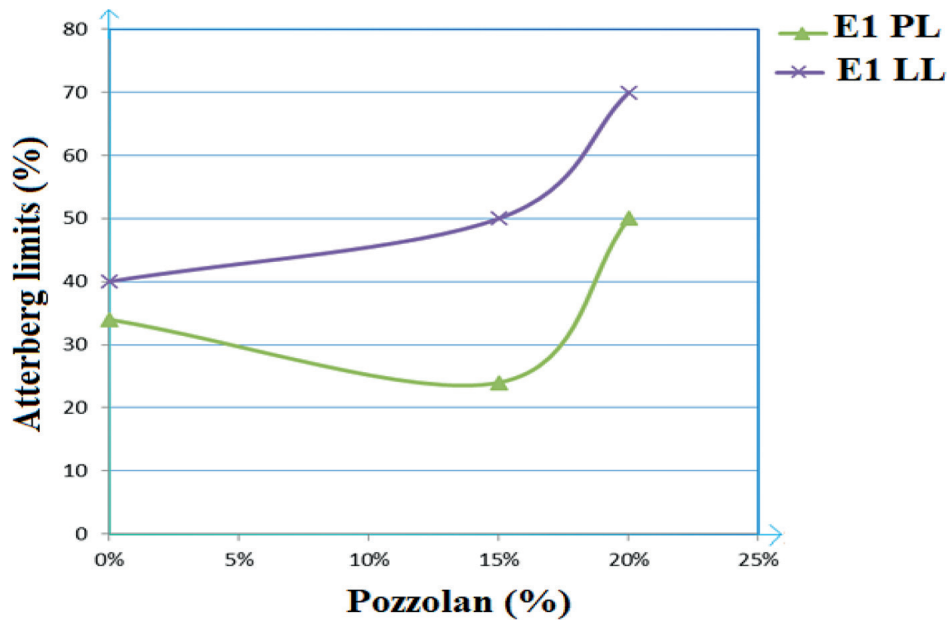


Figure 8. Atterberg limits (PL – plastic limit, LL – liquid limit)

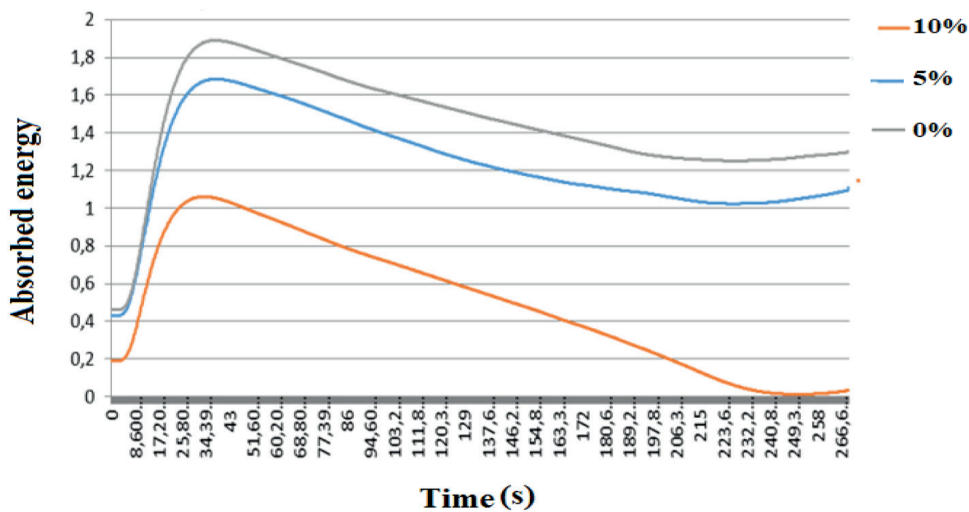


Figure 9. Result of the differential scanning calorimetry test

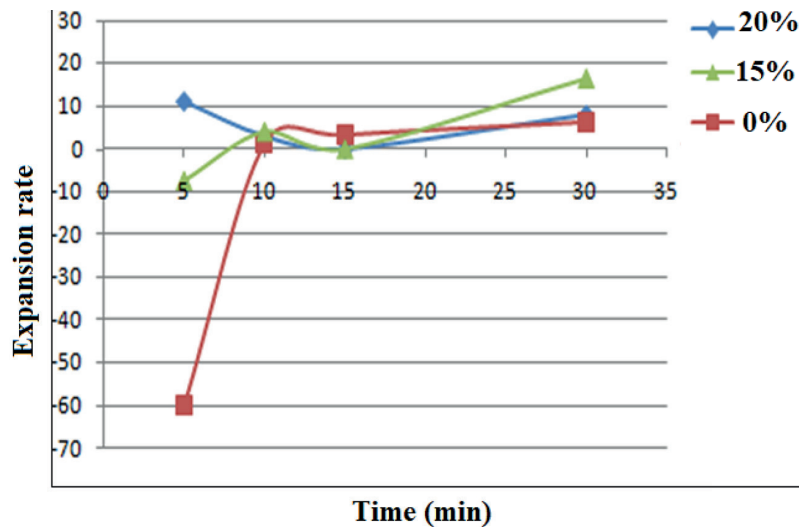


Figure 10. Diameter of expanded clay aggregate as a function of firing time

are all lower than  $1800 \text{ kg/m}^3$  [Ye et al., 1992], in agreement with several studies performed by other authors [Samson et al., 2017; Vandanapu et al., 2018]. The lowest density is that of 50% ECA which reaches  $1671 \text{ kg/m}^3$  [Kan et al., 2009].

*Water absorption*

The water absorption informs us about the open porosity of the specimen [Raimondo et al., 2009]. Therefore, Figure 12 shows the values of absorption of lightweight concrete as a function of percentage of ECA added. This figure reveals that the concrete doped with 50% of aggregate has a maximum value 14%, while these percentages of absorption are low, testifying to a good mechanical strength [Tharakarama et al., 2017].

**Mechanical analysis**

*Flexural strength*

Figure 13 shows the specimens made from the mixture of different percentage of expanded clay aggregate (0, 5, 10, 20, 30, 40 and 50%). The following test is designed to determine the required proportion of expanded aggregates that must be added to the lightweight concrete mix to ensure satisfactory strength according to US construction standards. Flexural strength is carried out on the specimens composed of (cement + sand + expanded clay aggregate). The unreinforced lightweight concrete is marked by the failure of the matrix [Melanie, 2003]. When the concrete could no longer resist the stress, the micro-cracks widened

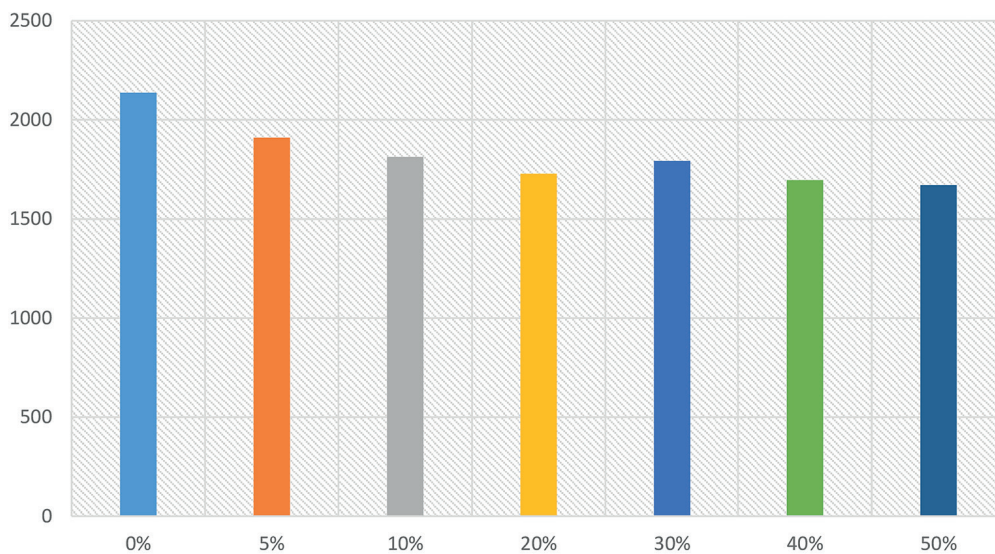
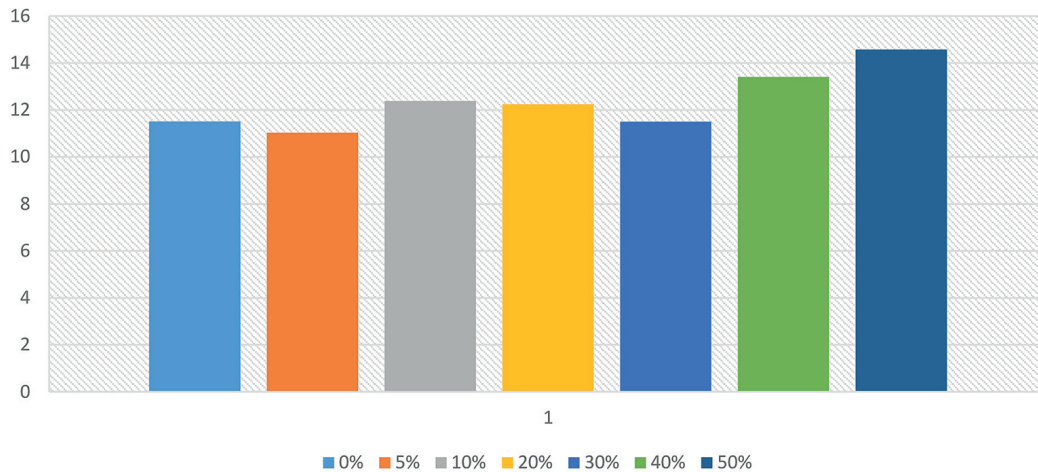
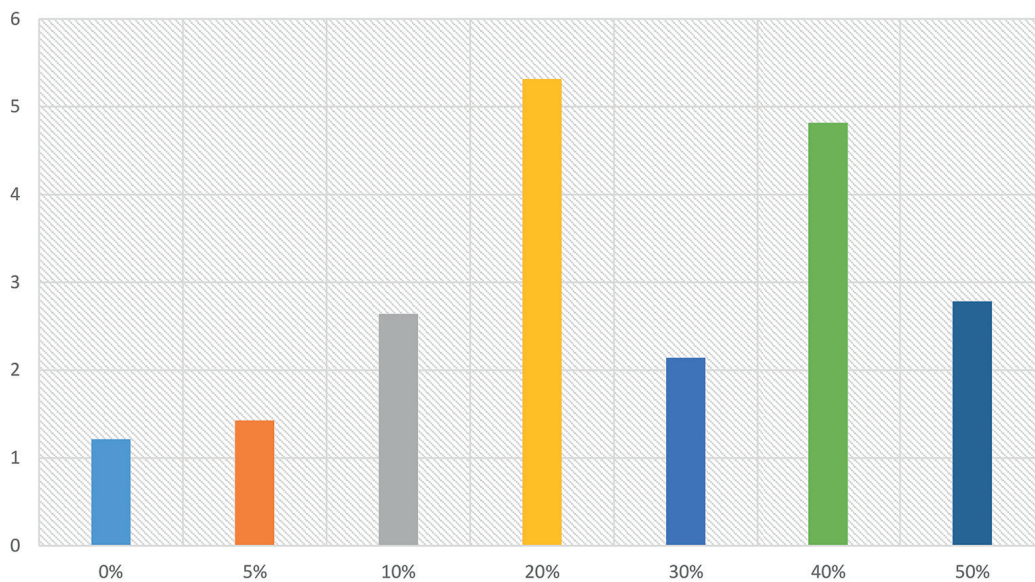


Figure 11. Density of cement samples with percentages of ECA added





**Figure 12.** Water absorption of samples



**Figure 13.** Flexural strength curves of lightweight concrete doped with expanded clay aggregate

and turned into macro-cracks [Wong et al., 2022]. It was noticed that the mechanical resistance increases with the percentage of expanded clay aggregate added until 40%. The highest resistance is observed in the mixture of 20% of clay aggregate added. It is apparent that with the increase of the percentage of expanded clay aggregate the density decreases as well as the strength increases. This is mainly due to the semi-porous surface and the pozzolanic activity of the studied aggregates with the cementitious matrix which reinforces the structure of the lightweight concrete [Awoyera et al., 2018; Wasserman et al., 1997]. The results of the maximum bending stresses of the specimens containing 20% aggregate which reached 5.31 Mpa and a density of 1728 kg/m<sup>3</sup>, can be used for splitting concrete according to the research

already carried out by others authors [Zhang et al., 1991; Wilson et al., 1988].

## CONCLUSIONS

This study allowed concluding the following. The mixture of marl and 15% pozzolan has the best expansion result (16.8%), and the lowest density of 1232 kg/m<sup>3</sup> according to the international standard. The decrease in absorbed energy is proportional to the increase in the percentage of pozzolan added. The density of the concrete decreases with the amount of aggregates added and reaches its minimum at 1671 kg/m<sup>3</sup> at 50% expanded clay aggregate. Flexural tests show the increase in mechanical strength as a function of

the amount of expanded clay aggregate added. The maximum strength was found in the mixture containing 20% of clay aggregate added.

## REFERENCES

1. Leblanc D., Olivier P. 1984. Role of strike-slip faults in the Betic-Rifian orogeny. *Tectonophysics*, 101(3–4), 345–355.
2. Tejera de Leon J., Boutakiout M., Ammar A., Ait Brahim L., El Hatimi N. 1995. The Central Rif Basins (Morocco); markers of out-of-sequence thrusting of terminal Miocene age in the core of the chain. *The Bulletin of the Geological Society of France*, 166(6), 751–761.
3. Durand M. 1972. Geotechnical properties of marls and clays from the Upper Triassic of Lorraine. Ph.D. Thesis, Henri Poincaré University, Nancy.
4. Reynolds R.C. 1980. Interstratified clay minerals.
5. Grim R.E. 1953. *Clay mineralogy*, 76(4), 317, LWW.
6. Mesrar, L., ELarousi, O., Lakrim, M., Jabrane, R. 2011. Characterization of miocenous marnes in the fes region before and after doping with manganese oxide (MnO<sub>2</sub>). *Geomaghreb*, 7, 13–20.
7. Allison L.E., Moodie C.D. 1965. Carbonate. *Methods of Soil Analysis: Part 2 Chemical and Microbiological Properties*, 9, 1379–1396.
8. Mesrar, L., Benamar, A., Mesrar, H., Jabrane, R. 2021. Physical and Mechanical Properties Improvement of Miocene Marls (Morocco) Doped by Iron Oxide Fe<sub>2</sub>O<sub>3</sub>. In: *Sustainable Environment and Infrastructure*. Springer, Cham, 259–269.
9. Mesrar L., Mesrar H., Jabrane R. 2014. Preparation and characterization of Miocene clay powders in the region of Fez (Morocco) after doping with metal oxides Al<sub>2</sub>O<sub>3</sub>. *Journal of Computer Science and Engineering Research (JCSER)*, (2), 1–4.
10. Yew M.K., Yew M.C., Han Beh J., Saw L.H., Lee F.W., Lee Y.L. 2021. Mechanical properties of barchip polypropylene fibre-reinforced lightweight concrete made with recycled crushed lightweight expanded clay aggregate. *Frontiers in Materials*, 410.
11. Becker P.F.B., Effting C., Schackow A. 2022. Lightweight thermal insulating coating mortars with aerogel, EPS, and vermiculite for energy conservation in buildings. *Cement and Concrete Composites*, 125, 104283.
12. Ye P., Chen Z., Su W. 2022. Mechanical properties of fully recycled coarse aggregate concrete with polypropylene fiber. *Case Studies in Construction Materials*, 01352.
13. Zhang M.H., Gjorv O.E. 1992. Penetration of cement paste into lightweight aggregate, *Cement and Concrete Research*, 22(1), 47–55.
14. Wasserman R., Bentur A. 1997. Effect of lightweight fly ash aggregate microstructure on the strength of concretes. *Cement and Concrete Research*, 27(4), 525–537.
15. Akwilapo L.D., Wiik K. 2003. Ceramic properties of Pugu kaolin clays. Part I: Porosity and modulus of rupture. *Bulletin of the Chemical Society of Ethiopia*, 17, 2.
16. Azarhomayun F., Haji M., Kioumars M., Shekarchi M. 2022. Effect of calcium stearate and aluminum powder on free and restrained drying shrinkage, crack characteristic and mechanical properties of concrete. *Cement and Concrete Composites*, 125, 104276.
17. Güneyisi E., Gesoğlu M., Karaoğlu S., Mermerdaş K. 2012. Strength, permeability and shrinkage cracking of silica fume and metakaolin concretes. *Construction and Building Materials*, 34, 120–130.
18. Bheel N., Kumar A., Shahzaib J., Ali Z., Ali M. 2021. An investigation on fresh and hardened properties of concrete blended with rice husk ash as cementitious ingredient and coal bottom ash as sand replacement material. *Silicon*, 1–12.
19. Wong L.S., Chandran S.N., Rajasekar R.R., Kong S.Y. 2022. Pozzolanic characterization of waste newspaper ash as a supplementary cementing material of concrete cylinders. *Case Studies in Construction Materials*, 01342.
20. Khudhair M.H., Elyoubi M.S., Elharfi A. 2018. New eco-friendly hydraulic binder based on a combination of inorganic additions and organic admixture: Formulation and Characterization. *Moroccan Journal of Chemistry*, 6(2), 259–271.
21. Khudhair M.H., Elyoubi M.S., Elharfi A. 2017. Comparative study of the influence of inorganic additions on the physical-chemical properties and mechanical performance of mortar and/or concrete. *Moroccan Journal of Chemistry*, 5(3), 493–504.
22. Alireza H., Adedapo M.A., Aniekan E.D. 2021. Ductility and flexure of lightweight expanded clay basalt fiber reinforced concrete slab. *Structural mechanics of engineering structures and constructions*, 17(1), 74–81.
23. Musial M.P., Grzymiski F., Trapko T. 2021. The effect of the pre-wetting of expanded clay aggregate on the freeze-thaw resistance of the expanded clay aggregate concrete. *Studia Geotechnica and Mechanica*, 43(2), 65–73.
24. Ghorbani A., Rabanifar H. 2021. The Effect of Lightweight Expanded Clay Aggregate on the Mitigation of Liquefaction in Shaking Table. *Geotechnical and Geological Engineering*, 39(3), 1861–1875.
25. Baronet J., Sorelli L., Charron J. P., Vandamme M., Sanahuja J. 2022. A two-scale method to rapidly characterize the logarithmic basic creep of concrete

- by coupling microindentation and uniaxial compression creep test. *Cement and Concrete Composites*, 125, 104274.
26. Melanie S. 2003. Elastic compatibility, mechanical behaviour and optimisation of lightweight aggregate concretes, Ph.D. Thesis, Laval University, Quebec.
  27. Bogas J.A., Gomes M.G., Real S. 2014. Bonding of steel reinforcement in structural expanded clay lightweight aggregate concrete: The influence of failure mechanism and concrete composition, *Construction and Building Materials*, 65, 350–359.
  28. Wang Y., Zhang S., Niu D., Fu Q. 2022. Quantitative evaluation of the characteristics of air voids and their relationship with the permeability and salt freeze–thaw resistance of hybrid steel–polypropylene fiber–reinforced concrete composites. *Cement and Concrete Composites*, 125, 104292.
  29. Zheng F., Hong S., Hou D., Dong B., Kong Z., Jiang R. 2021. Rapid visualization and quantification of water penetration into cement paste through cracks with X-ray imaging. *Cement and Concrete Composites*, 104293.
  30. Kornmann X., Rees M., Thomann Y., Necola A., Barbezat M., Thomann R. 2005. Epoxy-layered silicate nanocomposites as matrix in glass fibre-reinforced composites. *Composites Science and Technology*, 65(14), 2259–2268.
  31. Arib A., Sarhiri A., Moussa R., Remmal T., Gomi-na M. 2007. Caractéristiques structurales et mécaniques de céramiques à base d’argiles: influence de la source de feldspath. *Comptes Rendus Chimie*, 10(6), 502–510.
  32. Nshimiyimana P., Fagel N., Messan A., Wetschondo D. O., Courard L. 2020. Physico-chemical and mineralogical characterization of clay materials suitable for production of stabilized compressed earth blocks. *Construction and Building Materials*, 241, 118097.
  33. Pimraksa K., Chindaprasirt P. 2009. Lightweight bricks made of diatomaceous earth, lime and gypsum. *Ceramics International*, 35(1), 471–478.
  34. Silva V.M.D., Góis L.C., Duarte J.B., Silva J.B.D., Acchar W. 2014. Incorporation of ceramic waste into binary and ternary soil–cement formulations for the production of solid bricks. *Materials Research*, 17, 326–331.
  35. Aineto M., Acosta A., Iglesias I. 2006. The role of a coal gasification fly ash as clay additive in building ceramic. *Journal of the European Ceramic Society*, 26(16), 3783–3787.
  36. James J., Pandian P.K. 2018. Strength and micro-structure of micro ceramic dust admixed lime stabilized soil. *Revista de la Construcción. Journal of Construction*, 17(1), 5–22.
  37. Matias G., Faria P., Torres I. 2014. Lime mortars with heat treated clays and ceramic waste: A review. *Construction and Building Materials*, 73, 125–136.
  38. Li L., Liu W., You Q., Chen M., Zeng Q. 2020. Waste ceramic powder as a pozzolanic supplementary filler of cement for developing sustainable building materials. *Journal of Cleaner Production*, 259, 120853.
  39. Nie L., Zhang Y. 2011. Study on the application of lightweight aggregate ceramsite concrete in building. In: *Applied Mechanics and Materials*. Trans Tech Publications Ltd, 573–576.
  40. Mydin M.O., Sahidun N.S., Yusof M.M., Noordin N.M. 2015. Compressive, flexural and splitting tensile strengths of lightweight foamed concrete with inclusion of steel fibre. *Jurnal Teknologi*, 75(5).
  41. Samson G., Phelipot-Mardelé A., Lanos C. 2017. A review of thermomechanical properties of lightweight concrete. *Magazine of Concrete Research*, 69(4), 201–216.
  42. Vandanapu S.N., Krishnamurthy M. 2018. Seismic performance of lightweight concrete structures. *Advances in Civil Engineering*.
  43. Kan A., Demirboğa R. 2009. A novel material for lightweight concrete production. *Cement and Concrete Composites*, 31(7), 489–495.
  44. Raimondo M., Dondi M., Gardini D., Guarini G., Mazzanti F. 2009. Predicting the initial rate of water absorption in clay bricks. *Construction and Building Materials*, 23(7), 2623–2630.
  45. Tharakarama T., Veni B., Krishna P.B. 2017. An experimental investigation on light weight foam cement blocks with quarry dust replacement for fine aggregate. *Int. Res. J. Eng. Technol*, 4, 844–850.
  46. Awoyera P.O., Akinmusuru J.O., Dawson A.R., Ndambuki J.M., Thom N.H. 2018. Microstructural characteristics, porosity and strength development in ceramic-laterized concrete. *Cement and Concrete Composites*, 86, 224–237.
  47. Zhang M.H., Gjvovr O.E. 1991. Mechanical properties of high-strength lightweight concrete. *Materials Journal*, 88(3), 240–247.
  48. Wilson H.S., Malhotra V.M. 1988. Development of high strength lightweight concrete for structural applications. *International Journal of Cement Composites and Lightweight Concrete*, 10(2), 79–90.